Numerical analysis of the resonance mechanism of the lumped parameter system model for acoustic mine detection*

Wang Chi(王 驰)†, Zhou Yu-Qiu(周瑜秋), Shen Gao-Wei(沈高炜), Wu Wen-Wen(吴文雯), and Ding Wei(丁 卫)

Department of Precision Mechanical Engineering, Shanghai University, Shanghai 200072, *China*

(Received 23 February 2013; revised manuscript received 19 April 2013)

The method of numerical analysis is employed to study the resonance mechanism of the lumped parameter system model for acoustic mine detection. Based on the basic principle of the acoustic resonance technique for mine detection and the characteristics of low-frequency acoustics, the "soil-mine" system could be equivalent to a damping "mass-spring" resonance model with a lumped parameter analysis method. The dynamic simulation software, Adams, is adopted to analyze the lumped parameter system model numerically. The simulated resonance frequency and anti-resonance frequency are 151 Hz and 512 Hz respectively, basically in agreement with the published resonance frequency of 155 Hz and anti-resonance frequency of 513 Hz, which were measured in the experiment. Therefore, the technique of numerical simulation is validated to have the potential for analyzing the acoustic mine detection model quantitatively. The influences of the soil and mine parameters on the resonance characteristics of the soil–mine system could be investigated by changing the parameter setup in a flexible manner.

Keywords: acoustic mine detection, acoustic–seismic coupling, resonance model

PACS: 46.40.–f, 46.40.Ff, 43.20.+g, 43.40.+s **DOI:** 10.1088/1674-1056/22/12/124601

1. Introduction

Based on the mine mechanical property of big acoustic compliance and the acoustic-to-seismic coupling principle, the acoustic resonance technique has been validated to be a safe and reliable method of detecting non-metallic mines. Seismic waves may be induced and propagated into the soil under the vibration of the ground surface by exciting the low-frequency (< 1 kHz) acoustic waves to the multiphase porous soil medium. The seismic waves will be reflected and scattered back to the surface when meeting with buried objects like mines; in this way, the mine, which features big compliance, together with the soil on it will form a "mass-spring" system that will resonate. As a result, the vibration of the ground surface will change obviously and distinctively. By detecting the changes in the vibration of the ground surface, we can judge the existence of mines and do research on the acoustic imaging of mines.

Although the acoustic resonance technique demonstrates a promising prospect for detecting buried mines under laboratory conditions, we still have a lot to do to develop a practical engineering system for acoustic mine detection. Among others, it is necessary to further study the theoretical model of acoustic mine detection. Since 1999, Sabatier and Xiang,[1] Xiang and Sabatier,[2] and Donskoy *et al.*[3,4] have preliminarily established the linear and nonlinear resonance theoretical models for acoustic mine detection, by means of the lumped parameter system model based on the low-frequency acoustic characteristics and their research on the acoustic-to-seismic coupling principle for years. Meanwhile, they have carried out corresponding validation on their theoretical models. However, they failed to take into consideration the mine anti-resonance effect that could weaken the vibration of the ground surface in the study of the mechanical characteristic parameter of mines. In 2002, Yu *et al.*[5] investigated the anti-resonance mechanism of mines and validated it with the help of the experimental data from Sabatier. However, the anti-resonance effect appears to be very weak and it is not sufficient to represent the mine mechanical features. In 2005, Zagrai *et al.*[6] published a paper to discuss the mine multi-modal resonance phenomenon. According to the above theoretical and experimental studies, mines have a resonance phenomenon, and an anti-resonance and multi-modal resonance phenomena as well. Since 2008, the solution method of frequency response functions has been adopted to analyze the resonance, anti-resonance, and multi-modal resonance mechanisms of mines qualitatively in a unified manner in Refs. [7]–[9]. However, the method may not be used to study the resonance frequencies of the acoustic resonance mine detection model and their influencing factors quantitatively. In recent years, some papers have been published about theoretical and experimental studies of acoustic mine detection, as described in Refs. [10]–[13], such as the study of the cepstral approach,

*Project supported, in part, by the National Natural Science Foundation of China (Grant No. 41104065), the "Chen Guang" Program of Shanghai Municipal Education Commission and Shanghai Education Development Foundation, China (Grant No. 12CG047), the Scientific Research Innovation Program of Shanghai Municipal Education Commission, China (Grant No. 13YZ022), and the State Key Laboratory of Precision Measuring Technology and Instruments, China.

†Corresponding author. E-mail: wangchi@shu.edu.cn

© 2013 Chinese Physical Society and IOP Publishing Ltd

Green's functions, laser-acoustic system, etc.

Based on study, the resonance mechanism of the "soil–mine" system is found to be an important theoretical foundation to describe the mechanical characteristics of mines, which affects the acoustic imaging of mines. The analysis of the resonance mechanism of the "soil–mine" system quantitatively is helpful for developing the practical engineering system for acoustic mine detection and also for seeking methods to improve the system sensitivity. In this paper, a numerical simulation technique based on Adams, the software of automatic dynamic analysis of mechanical systems, is proposed to investigate the lumped parameter system model for acoustic mine detection in a simulative manner and to analyze the resonance mechanism of the system and their influencing factors quantitatively. The simulation results accord well with the published experimental data, which verifies the feasibility of the method proposed in this paper.

2. Basic principle of the acoustic resonance technique for mine detection

The acoustic resonance technique for detecting buried mines is mainly based on the acoustic-to-seismic coupling principle and the mechanical characteristics of a big mine compliance. According to Refs. [14]–[18], as shown in Fig. 1, when the airborne low-frequency (below several kHz) acoustic waves are radiated into the multiphase medium (i.e., surface soil) that is composed of a solid phase and a fluid phase (e.g., air and water), some of the energy is coupled into the ground because of the small impedance difference between the air and the fluid phase of soil, although most of the energy is reflected back to the air due to the big impedance difference between the air and the solid phase of surface soil. As a result, the vibration of the ground surface is induced and various coupled seismic waves are produced due to the effect of momentum and viscous friction between the solid phase and fluid phase, including the Rayleigh wave, shear wave, fast compressional wave (i.e., fast P-wave), and slow compressional wave (i.e., slow P-wave), etc. The Rayleigh wave, fast P-wave, and shear wave will cause a strong solid phase vibration compared with the weak fluid phase vibration, that is to say, their energy attenuation coefficients are small in the solid phase compared with in the fluid phase of soil. As a result, these seismic waves may penetrate through mines that they meet with due to the small acoustic impedance difference between the solid phase of soil and the mine casing. This means that only a small portion of seismic energy is reflected or scattered back to the ground surface. The slow P-wave will cause a strong fluid phase vibration and weak solid phase vibration of soil, that is to say, it has a large attenuation coefficient in the solid phase compared with in the fluid phase of soil. As a result, the slow P-wave will be strongly reflected or scattered to the ground surface due to the large acoustic impedance difference between the fluid phase of the soil and the mine casing.

The propagation depth of the slow P-wave is limited due to its high dispersivity during propagation that will result in a big energy attenuation coefficient within the soil. As a result, the ground vibration changes insignificantly and thus the existence of a buried object (e.g. a landmine) cannot be judged. However, a landmine has a big acoustic compliance compared with the surrounding soil due to its unique structure composed of a container, a fuze, and an air cavity. Therefore, the mine and the soil on it will form a "mass–spring" resonance system. The "soil–mine" system will resonate with the excitation of the coupled seismic waves, especially the P-slow wave, which leads to a significant increase of the reflected or scattered seismic waves. Thus, an obvious and unique change will occur in the ground surface vibration above the mine. In this way, we can study the buried mine's acoustic imaging.

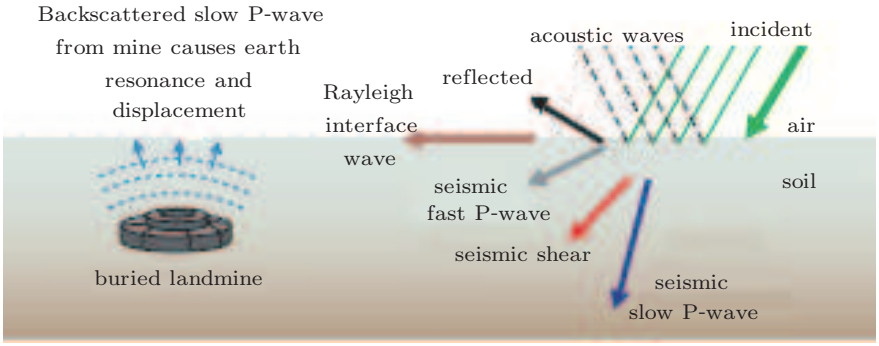


Fig. 1. (color online) Schematic diagram of the acoustic-to-seismic coupling and the mine resonance.[14–18]

3. Numerical analysis of the acoustic mine detection model

Generally, the dimensions of an antipersonnel mine are 5 cm $\sim$ 10 cm and its buried depth is about 5 cm. The dimensions of an antitank mine are 20 cm–30 cm and its buried depth is about 20 cm. According to the fundamental principle of the acoustic resonance mine detection technique and the properties of low-frequency acoustics, the size, and buried depth of a

mine are both close to the wavelength of the acoustic wave of the frequency below 1 kHz. Therefore, the lumped parameter system model can be used to analyze the "soil–mine" system, which is composed of a compliant mine and the soil on it. The continuous "soil–mine" system can be simplified into a corresponding discrete element system with equivalent physical parameters or characteristics. The mine can be equivalent to a mass–spring due to its great compliance coefficient compared with that of the surrounding soil; the soil on the mine can be equivalent to an elastic mass block. In addition, the coupled seismic waves attenuate during their propagation in soil, resulting from the viscous friction and dispersive effect. Therefore, the "soil–mine" system is a complicated damping resonance system with multi-degrees of freedom. Figure 2 shows a classic simplified "soil–mine" resonance system model,[1–5] where m_1 represents the mass of the soil on the mine and m_2 is the mass of the upper diaphragm of the mine; k_1 and k_2 denote the equivalent spring stiffness factors due to the shear force and normal stress of soil respectively; k_3 is the equivalent spring stiffness factor of the mine diaphragm; c_1 and c_2 are respectively damping coefficients due to the shear force and compression of soil; c_3 represents the mine damping coefficient.

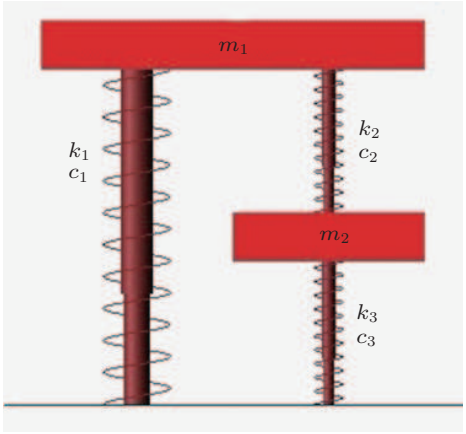


Fig. 2. (color online) Schematic diagram of the soil–mine resonance system model.[1–5]

According to the "soil–mine" resonance system model shown in Fig. 2 and linear vibration theory, we can obtain the following expression:[13]

$$M\ddot{X} + C\dot{X} + KX = F, \tag{1}$$

where $X = \mathrm{diag}(x_1, x_2)$ is a displacement matrix dependent on the ground surface and mine; $\dot{X}$ and $\ddot{X}$ are respectively velocity and acceleration matrixes; $M = \mathrm{diag}(m_1, m_2)$ is a mass matrix, $C = \begin{pmatrix} c_1 + c_2, -c_2 \\ -c_2, c_2 + c_3 \end{pmatrix}$ is a damping coefficient matrix; $K = \begin{pmatrix} k_1 + k_2, -k_2 \\ -k_2, k_2 + k_3 \end{pmatrix}$ is a stiffness matrix; $F = \mathrm{diag}(F, 0)$ is an applied external force matrix. By ignoring the effect of damping, the natural resonance frequency can be derived as follows:

$$\omega_{\mathrm{f}}^2 = \frac{1}{2}\left(\frac{k_{12}m_2 + k_{23}m_1}{m_1 m_2}\right) \mp \frac{1}{2}\left[\left(\frac{k_{12}m_2 + k_{23}m_1}{m_1 m_2}\right)^2 - 4\left(\frac{k_{12}k_{23} - k_2^2}{m_1 m_2}\right)\right]^{1/2}. \tag{2}$$

According to Ref. [5], the anti-resonance frequency can be expressed as

$$\omega_{\mathrm{anti}} = \sqrt{(k_2 + k_3)/m_2}. \tag{3}$$

Listed in Table 1 are the related experimental parameter data of the soil and mines provided in Ref. [3]. According to Eqs. (2) and (3), the measured resonance frequency is 155 Hz. The anti-resonance frequency is 513 Hz based on Ref. [5]. For different mines and soils, the "soil–mine" system has different resonance frequencies. The soils are different in different countries or regions, or even at different locations in the same mine field. Therefore, it is very difficult or even impossible to exactly analyze the mechanical properties of mines buried in different mine fields in a sampling experiment. For this reason, the technique of numerical simulation is proposed in this paper to study the "soil–mine" resonance system model quantitatively and to provide the technical and theoretical basis for obtaining mechanical characteristic parameters of mines (e.g. resonance frequency).

Table 1. Soil and mine parameters for simulation.[3]

Parameters of mine (VS-1.6)			Parameters of soil (buried depth of 25 mm)				
m_2/(kg/m^2)	c_3/(kg/(m^2·s))	k_3/(Pa/m)	m_1/(kg/m^2)	c_2/(kg/(m^2·s))	k_2/(Pa/m)	c_1/(kg/(m^2·s))	k_1/(Pa/m)
12	1700	2.5×10^7	40	4000	1×10^8	3900	2.4×10^7

Adams, the software for automatic dynamic analysis of mechanical systems, is a virtual prototype analysis software developed by Mechanical Dynamics Inc. (MDI). Users can use the software to model and test a mechanical vibration system on a computer and then investigate the vibration performance of a complex mechanical system by adjusting parameters in a flexible manner. The model shown in Fig. 2 can be simulated easily according to the relative parameters shown in Table 1. According to the theory of mechanical vibration, the relation between the response output speed $v(\mathrm{j}\omega)$

and the applied input force $F(\mathrm{j}\omega)$ can be described by the expression: $v(\mathrm{j}\omega) = F(\mathrm{j}\omega)H(\mathrm{j}\omega)$. Therefore, the velocity frequency response function is $H(\mathrm{j}\omega) = v(\mathrm{j}\omega)/F(\mathrm{j}\omega)$. The simulating magnitude spectrum curve of the ground surface vibration velocity is shown in Fig. 3. The horizontal ordinate denotes the frequency ($f = \omega/2\pi$) and the vertical ordinate $20\lg(|H(\mathrm{j}\omega)|)$. From Fig. 3, we can find that the resonance frequency and anti-resonance frequency are 151 Hz and 512 Hz respectively, which are basically consistent with the measured resonance frequency of 155 Hz and anti-resonance frequency of 512 Hz given in Refs. [3] and [5] mentioned above. Therefore, the proposed numerical analysis in this paper is validated as being a feasible potential.

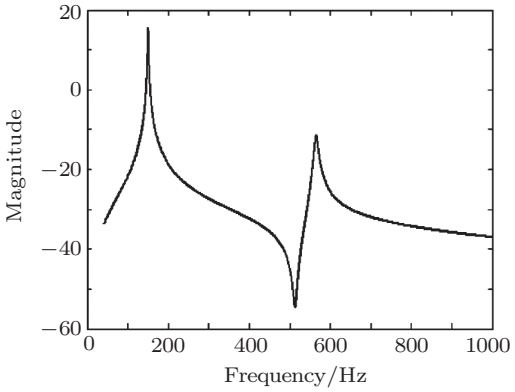


Fig. 3. Magnitude spectrum curve of the ground surface (m_1) vibration velocity.

4. Influencing factors of the soil–mine resonance system

Different environmental parameters, e.g., the buried depth, porosity and moisture of the soil, will lead to different values of soil mass m_1, soil shear stiffness k_1, the soil shear damping coefficient c_1, soil compression stiffness k_2, and the soil compression damping coefficient c_2. Similarly, different types of mines will have different values of mine mass m_2, mine damping coefficient c_3, and mine stiffness k_3. It is obvious that both the mine and the soil parameters influence the resonance characteristics of the soil–mine system. In the following part, the software, Adams, is used to analyze the effects of these different parameters comprehensively. It should be noted that the relative parameters of mine and soil are selected from Table 1. During analyzing the influence of a parameter (e.g. the soil shear stiffness, k_1), different values may be given to the parameter while other parameters are kept unchanged.

4.1. Effect of soil shear parameters

Figure 4 shows the influences of soil shear stiffness k_1 on system resonance characteristics. As shown in Fig. 4, the resonance frequency increases as the soil shear stiffness k_1 increases, while the anti-resonance frequency remains the same. It should be noted that the soil shear stiffness k_1 has little influence on the surface vibration amplitude at a low resonance frequency. These results are consistent with the experimental results published in Ref. [6]. As a matter of fact, by using the analytical method of electromechanical analogy, the stiffness is equivalent to capacitance and the mass is equivalent to inductance. The vibration energy just exchanges between capacitance and inductance. Therefore, the soil shear stiffness k_1 has no effect on the vibration amplitude.

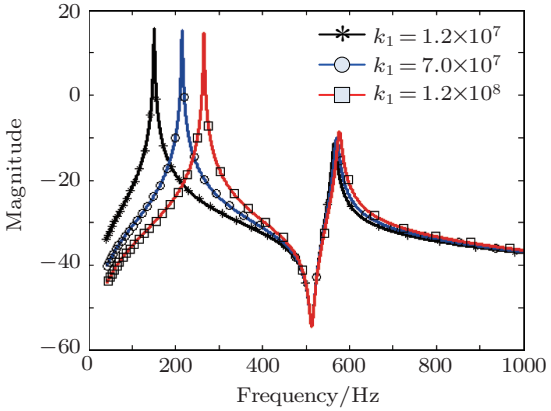


Fig. 4. (color online) Effects of the soil shear stiffness on system resonance characteristics.

Figure 5 shows the effects of the soil shear damping coefficient c_1 on the system resonance characteristics. As shown in Fig. 5, the shear damping coefficient has little effect on the resonance frequency, but a strong influence on the vibration amplitude. The surface vibration amplitude decreases as the shear damping coefficient increases. The shear damping coefficient of soil results from the viscous friction among soil particles, which will lead to the seismic energy consumption that reduces the surface vibration amplitude. The larger the shear damping coefficient, the more the energy consumes. Therefore, the surface vibration amplitude decreases in the end.

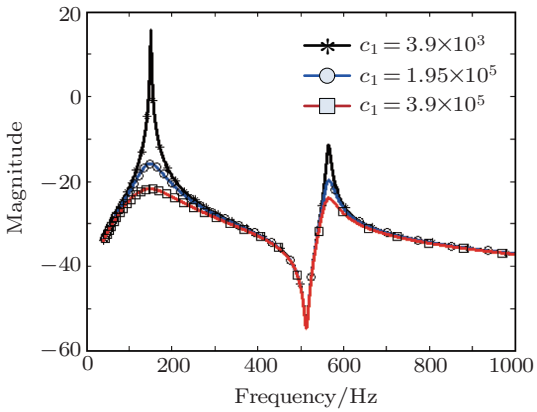


Fig. 5. (color online) Effects of the soil shear damping on the system resonance characteristics.

4.2. Effect of soil compression parameters

Figure 6 shows the effects of the soil compression stiffness on the system resonance characteristics. As shown in

Fig. 6, the resonance frequency decreases slightly as the soil compression stiffness decreases. Especially, the anti-resonance frequency and the surface vibration amplitude decrease dramatically as the soil compression stiffness decreases.

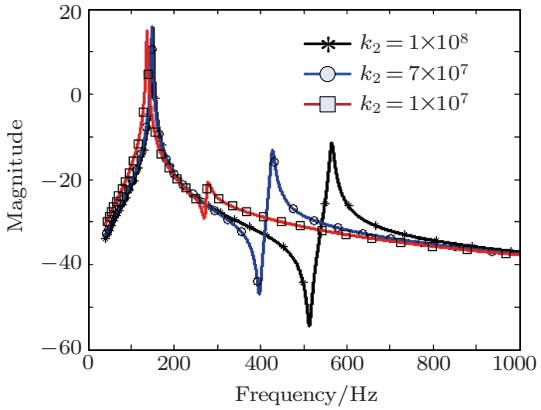


Fig. 6. (color online) Effects of the soil compression stiffness on the system resonance characteristics.

Figure 7 shows the effects of the soil compression damping coefficient on the system resonance characteristics. The influence mechanism is similar to that of the soil shear damping coefficient. The compression damping coefficient has little influence on the vibration amplitude. The compression damping coefficient is generated due to the viscous friction between the slow P-wave and soil particles, and the 'dragging' effect of liquid when the slow P-wave propagates in the soil–liquid phase. The soil compression damping coefficient influences the vibration amplitude. The larger the compression damping coefficient, the weaker the vibration amplitude will be.

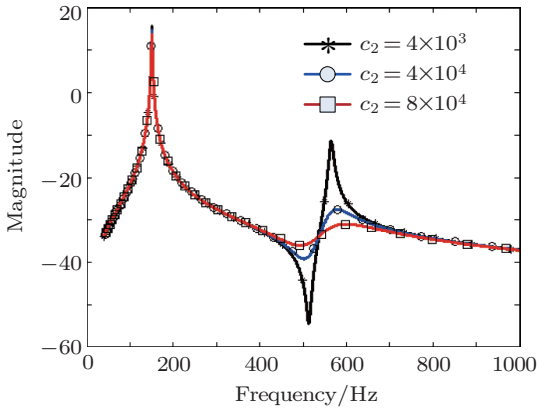


Fig. 7. (color online) Effects of the soil compression damping on the system resonance characteristics.

4.3. Effect of the buried depth of the mine

Figure 8 shows the effects of the soil mass m_1 on the top of a buried mine on the system resonance characteristics. As shown in Fig. 8, the resonance frequency decreases as the soil mass m_1 increases, whereas the anti-resonance frequency remains the same. In addition, in most of the frequency band, a bigger soil mass leads to a weaker vibration amplitude.

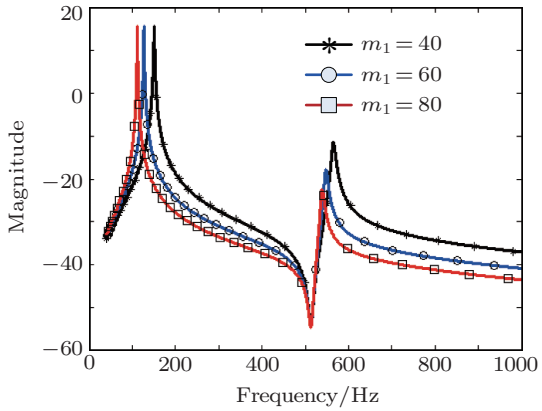


Fig. 8. (color online) Effects of the soil mass on the top of a mine on the system resonance characteristics.

Different buried depths of mines are equivalent to different soil masses on the top of mines. According to Ref. [19], the soil parameters vary with the buried depth H, and their relationship can be described as $m_1 \sim H$, $k_1 \sim H^{0.5}$, $k_2 \sim H^{-1}$, $c_1 \sim H$, and $c_2 \sim H$. Based on the proportionate relationships and the experimental parameters shown in Table 1, we can obtain the simulation results shown in Fig. 9 with the buried depth of H and the buried depth of $2H$. The soil mass on top of the mine and the damping coefficient increase as the buried depth increases, which means that the resonance frequency and the surface vibration magnitude will decrease, which is shown in Fig. 9. However, the effect of the soil shear stiffness k_1 can be ignored when the mine buried depth is very small. The soil compression stiffness and thus the anti-resonance frequency decreases with the increase of the mine's buried depth. The simulation results of different buried depths well accord with the experimental results published in Ref. [5].

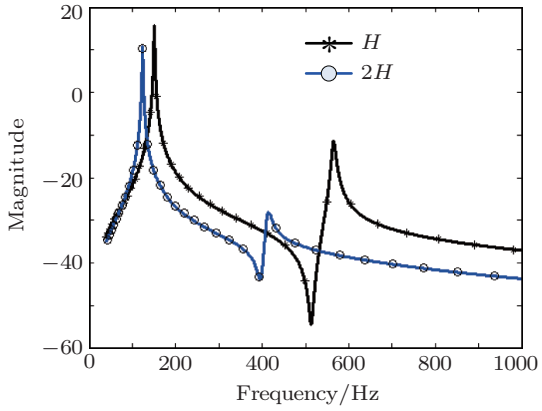


Fig. 9. (color online) Effects of the buried depth of the mine on the system resonance characteristics.

4.4. Effect of mine parameters

Different types of landmines have different values of mass, stiffness, and damping coefficients, thus producing different influences on the resonance characteristics of the soil–mine system. Figure 10 shows the influences of the mine upper diaphragm mass m_2 on the system resonance characteris-

tics. Figure 10 shows that the resonance frequency and the anti-resonance frequency decrease with the increase of mass m_2. However, the ground surface vibration amplitude changes slightly at low resonance frequency.

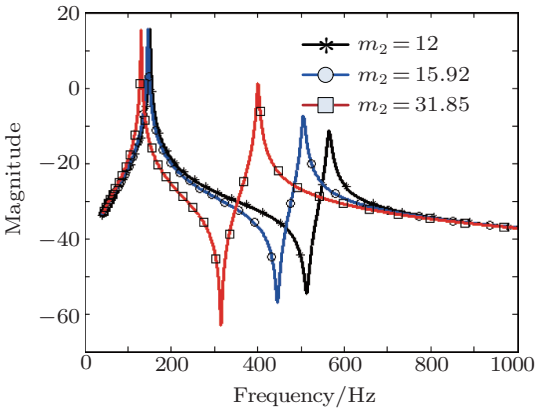


Fig. 10. (color online) Effects of the mine diaphragm mass on the system resonance characteristics.

Figure 11 shows the influence of mine stiffness k_3 on the system resonance characteristics. Both the resonance frequency and the anti-resonance frequency go upward as the stiffness k_3 increases. According to Eq. (3), the anti-resonance frequency can be calculated from the expression: $\omega = \sqrt{(k_2+k_3)/m_2}$. When the ratio of k_2/k_3 is very small, the anti-resonance frequency is approximately $\omega = \sqrt{k_3/m_2}$. Therefore, when the stiffness of the buried object, e.g., a rock or a sheet metal, is greater, the anti-resonance frequency determined by its stiffness is much greater than that of a buried mine. This means that the anti-resonance mechanism is suitable for the detection of buried mines.

Figure 12 shows the effects of the damping coefficient of a mine on the system resonance characteristics. Damping means an attribute of energy consumption. The energy consumption increases with the damping coefficient increasing, which leads to the decrease of the surface vibration amplitude. Similar to the effect of the soil damping coefficient, the surface vibration amplitude decreases and the resonance frequency remains the same as the mine damping coefficient increases.

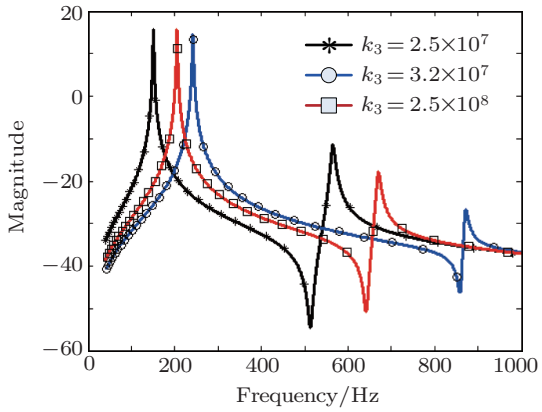


Fig. 11. (color online) Effects of the compression stiffness of a mine on the system resonance characteristics.

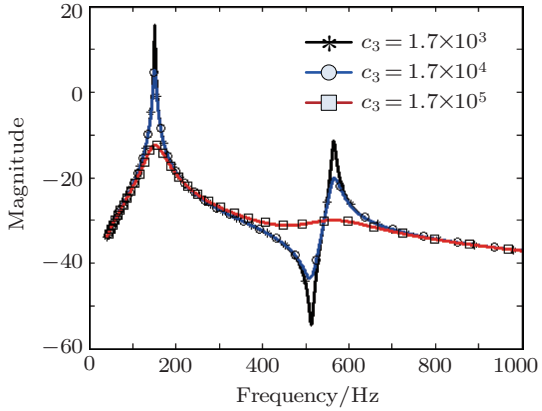


Fig. 12. (color online) Effects of the damping of a landmine on the system resonance characteristics.

Based on the above simulation results, when the relevant parameters of the soil and landmine increase, their effects on the resonance characteristics of the soil–mine system can be summarized in Table 2. The notation '↑' represents an increase, the notation '↓' a decrease, and the notation '–' represents an invariant.

Table 2. Effects of parameters of both soil and landmine to the resonance characteristics.

	Landmine			Soil				
	Mass	Damping	Stiffness	Mass	Shear damping	Compression damping	Shear stiffness	Compression stiffness
Parameter variation	↑	↑	↑	↑	↑	↑	↑	↑
Resonance frequency	↓	–	↑	↓	–	–	↑	↑
Anti-resonance frequency	↓	–	↑	–	–	–	–	↑

5. Conclusions

Based on the basic principle of acoustic resonance mine detection, a numerical simulation technique is proposed in this paper to study the multi-modal resonance phenomenon of the acoustic mine resonance mechanism in a quantitative way with the software, Adams. The simulation results are consistent with the previously published experimental data, which validates the feasibility of the numerical analysis technique. The influences of the parameters of the soil and the mine on the resonance characteristics of the soil–mine system are simulated, too. We can draw the following conclusions.

(i) If a mine's buried depth is small, the resonance frequency is influenced only by the values of the mass and the stiffness of the soil and the mine; the resonance frequency does

not vary with the damping coefficients of the soil and the mine.

(ii) The resonance frequency, anti-resonance frequency, and surface vibration amplitude decrease with the increase of the mass of the buried mine. The resonance frequency and anti-resonance frequency increase with the increase of the stiffness of the buried mine. The resonance frequency and anti-resonance frequency increase remain the same and the surface vibration amplitude decreases as the mine damping coefficient increases.

(iii) When the mass of the soil on the top of a buried mine increases, the resonance frequency and surface vibration amplitude decrease; the anti-resonance frequency remains the same. When the shear damping coefficient or compression damping coefficient increases, the resonance frequency and anti-resonance frequency remain the same while the surface vibration amplitude decreases. When the shear stiffness increases, the resonance frequency increases; the anti-resonance frequency and the surface vibration amplitude remain the same. When the compression stiffness increases, the resonance frequency and anti-resonance frequency increase correspondingly.

Some of the above conclusions are verified by experiments and some are predictive results. These simulation results provide a theoretical basis and method for further studying the theoretical model of acoustic mine detection. However, acoustic mine detection is a complex and difficult undertaking. Although the effects of such parameters as mass, damping and stiffness on the resonance characteristics of the soil–mine system are simulated, no investigation has been carried out into the relationships between the parameters and the more intuitive physical quantities, such as soil porosity, humidity, and density. In addition, there is a lack of detailed theoretical analysis and comprehensive experimental verification about the simulation results obtained in the paper. These relevant issues should be further explored in the future. For example, the research content and methods described in Refs. [20]–[25] could be used for further study, in addition to the experimental studies mentioned above in this paper.

References

[1] Sabatier J M and Xiang N 2001 *IEEE Trans. Geosci. Remote Sensing* **39** 1146

[2] Xiang N and Sabatier J M 2003 *J. Acoust. Soc. Am.* **113** 1333

[3] Donskoy D, Reznik A, Zagrai A and Ekimov A 2005 *J. Acoust. Soc. Am.* **117** 690

[4] Donskoy D 2008 *J. Acoust. Soc. Am.* **123** 3042

[5] Yu S H, Gandhe A, Witten T R and Mehra R K 2002 *Proceedings of SPIE* 4742*: Detection and Remediation Technologies for Mines and Minelike Targets VII*, April 1, 2002, Orlando, Florida, USA, p. 701

[6] Zagrai A, Donskoy D and Ekimov A 2005 *J. Acoust. Soc. Am.* **118** 3619

[7] Wang C, Liu Z G, Li X F, Sun F and Zhang G X 2008 *Acta Acustica* **33** 354 (in Chinese)

[8] Wang C, Li X F, Fu J, Li H Y, Liang G Q and Zhang G X 2008 *Opt. Precision Eng.* **16** 1716 (in Chinese)

[9] Wang C, Yu Y J, Li X F and Liang G Q 2010 *Acta Phys. Sin.* **59** 6319 (in Chinese)

[10] Khan U S, Al-Nuaimy W and El-Samie F E A 2010 *J. Vis. Commun. Image R.* **21** 731

[11] Zabolotskaya E A, Llinskii Y A, Hay T A and Hamilton M F 2012 *J. Acoust. Soc. Am.* **131** 1831

[12] Lancranjan I I, Miclos S, Savastru D, Savastru R and Opran C 2012 *Proceedings of SPIE* 8433: *Laser Sources and Applications*, April 16, 2012, Brussels, Belgium, article id. 843315

[13] Mao X, Li G Q, Wang C and Ding W 2012 *Prz. Elektrotechniczn* **88** 162

[14] Biot M A 1956 *J. Acoust. Soc. Am.* **28** 168

[15] Biot M A 1956 *J. Acoust. Soc. Am.* **28** 179

[16] Sabatier J M, Bass H E, Bolen L N, Attenborough K and Sastry V V S S 1986 *J. Acoust. Soc. Am.* **79** 1345

[17] Sabatier J M, Bass H E and Bolen L N 1986 *J. Acoust. Soc. Am.* **80** 646

[18] Robert W H and Kenneth D R 2005 *Linc. Lab. J.* **15** 3

[19] Donskoy D, Ekimov A, Sedunov N and Tsionskiy M 2002 *J. Acoust. Soc. Am.* **111** 2705

[20] Liu X B, Zhang J R and Li P 2012 *Chin. Phys. B* **21** 054301

[21] Huang B, Zhang Y L, Zhang D and Gong X F 2010 *Chin. Phys. B* **19** 054302

[22] Wu D, Tao C, Liu X J and Wang X D 2012 *Chin. Phys. B* **21** 014301

[23] Zheng H P, Jiang Y M, Peng Z and Fu L P 2012 *Acta Phys. Sin.* **61** 214502 (in Chinese)

[24] Zhang Q, Li Y C, Liu R, Jiang Y M and Hou M Y 2012 *Acta Phys. Sin.* **61** 234501 (in Chinese)

[25] Jian X H, Cui Y Y, Xiang Y J and Han Z L 2012 *Acta Phys. Sin*. **61** 217801 (in Chinese)